



Stripe domains in electrodeposited Ni₉₀Fe₁₀ thin films

N. Cotón^a, J.P. Andrés^b, E. Molina^a, M. Jaafar^c, R. Ranchal^{a,d,*}

^a Dpto. Física de Materiales, Fac. CC. Físicas, Universidad Complutense de Madrid, Ciudad Universitaria s/n, Madrid 28040, Spain

^b Univ. Castilla La Mancha, Inst. Reg. Invest. Cient. Aplicada IRICA, Dept. Appl. Phys., Ciudad Real 13071, Spain

^c Departamento de Física de la Materia Condensada and Condensed Matter Physics Center (IFIMAC), Universidad Autónoma de Madrid, Madrid, Spain

^d Instituto de Magnetismo Aplicado, UCM-ADIF-CSIC, Las Rozas 28232, Spain

ARTICLE INFO

Keywords:

Magnetic films and multilayers
Metals and alloys
Magnetostriction
Magnetic measurements

ABSTRACT

Here we have investigated the formation of stripe domains in electrodeposited Ni₉₀Fe₁₀ films, a metallic alloy with relevant magnetoelastic properties. The X-ray diffractometry patterns confirm the deposition of NiFe with an experimental lattice parameter close to the theoretical value. We have analyzed the influence of both magnetic stirring and an applied magnetic field perpendicular to the sample plane on the formation of stripe domains in Ni₉₀Fe₁₀ films. It is observed the characteristic fingerprint of stripe domains, i.e. the transcritical shape in the in-plane hysteresis loops when the electrolyte is not magnetically stirred during electrodeposition. The quality factor reveals a moderate perpendicular magnetic anisotropy which is confirmed by the stripe periodicity inferred by Magnetic Force Microscopy. In particular, stripe domains are only visible by this technique when the sample thickness is well above the theoretical critical thickness for the stripe domains to be formed. Finally, in samples released after being grown in outward bent flexible substrates it has been promoted an induced in-plane magnetoelastic magnetic anisotropy that reduces the perpendicular magnetic anisotropy. The high quality of the samples studied in this work from the magnetoelastic point of view is reflected by the magnetostriction constant of -22 ppm that it has been experimentally inferred.

1. Introduction

The interplay between magnetism and mechanical properties gives rise to magnetostriction [1,2]. One way to characterize magnetoelastic materials is by the magnetostriction constant (λ), that expresses the change of dimension when a magnetic material is magnetized:

$$\lambda = \frac{l - l_0}{l_0} \quad (1)$$

being l the length in the magnetic saturated state and l_0 the initial length, respectively. For the fabrication of miniaturized straintronic devices, there is nowadays a great interest in developing the same performance in nanometric magnetoelastic systems as in bulk materials. In addition, there is an increasing attention in magnetoelasticity since it can be exploited in spin waves generation [3–6]. Spin waves are collective excitations of the electron spin system, and they have been proposed for applications such as information transfer with low energy dissipation, high-speed technology or analog computing [3,7–10]. In that sense, spin textures play a fundamental role for the stabilization and manipulation of spin waves, and therefore, a huge effort is performing

for the development of tunable magnetic structures.

Stripe domains are among the spin textures capable to promote reproducible spin waves generation [11–14]. In materials with moderate perpendicular magnetic anisotropy (PMA), stripe domains are archetypical magnetic configurations that appear due to competing interactions because of the alternating up and down out-of-plane (OOP) orientation of the magnetization [15]. The quality factor (Q) gives an idea whether stripe domains can be expected or not in a material system [16]:

$$Q = K_U / 2\pi M_{sat}^2 \quad (2)$$

where K_U is the perpendicular magnetic anisotropy constant, and M_{sat} is the saturation magnetization. For materials with moderate or low PMA, i.e. $Q < 1$, stripe domains appear above a theoretical critical thickness (t_{cr}):

$$t_{cr} = 2\pi \sqrt{A_{ex} / K_U} \quad (3)$$

being A_{ex} the exchange energy per unit length. If $Q > 0.1$, stripe domains are wider than the layer thickness, whereas for $Q < 0.1$ they

* Corresponding author at: Dpto. Física de Materiales, Fac. CC. Físicas, Plaza de las Ciencias 1, Madrid 28040, Spain.

E-mail address: rociran@ucm.es (R. Ranchal).

<https://doi.org/10.1016/j.jmmm.2022.170246>

Received 13 October 2022; Received in revised form 21 November 2022; Accepted 28 November 2022

Available online 1 December 2022

0304-8853/© 2022 The Author(s). Published by Elsevier B.V. This is an open access article under the CC BY-NC-ND license (<http://creativecommons.org/licenses/by-nc-nd/4.0/>).

exhibit a periodicity equals to the layer thickness.

The family of Ni-Fe alloys is one of the most extensively studied ferromagnetic metallic systems due to the possibility of reaching small coercivity, large M_{sat} , and high permeability by means of composition and growth conditions. In $Ni_{80}Fe_{20}$ films, stripes have been observed because of columnar growth in sputtered layers [17] or have been promoted when coupled with other magnetic systems with large PMA as NdCo [18]. However, the null magnetostriction of $Ni_{80}Fe_{20}$ makes not possible to use it in magnetoelastic applications. $Ni_{90}Fe_{10}$ has been previously studied because of its magnetoelastic properties [19–20] since this composition exhibits a λ that can reach -20 ppm. In addition, evaporated $Ni_{90}Fe_{10}$ thin layers on top of Cu can show a large OOP magnetic anisotropy contribution due to mechanical strain [19].

The main goal of this work is to achieve high quality $Ni_{90}Fe_{10}$ magnetoelastic thin films with tunable stripe domains. We have studied the influence of growth conditions in terms of both magnetic stirring and an applied magnetic field on the magnetic properties of $Ni_{90}Fe_{10}$ electrodeposited layers. Also, we have inferred a λ of -22 ppm in these layers that reflects their high quality from the magnetoelastic point of view.

2. Experimental section

$Ni_{90}Fe_{10}$ layers were grown by electrodeposition on both glass (rigid) and kapton (flexible) substrates covered with a gold layer to increase the electrical conductivity of these two electrically insulating substrates. We have used a three-electrode cell with a platinum mesh as counter electrode and a Ag/AgCl (3 M NaCl) reference electrode. A PalmSens EmStat3 + Blue potentiostat was used to perform the depositions that were performed with (500 rpm) and without magnetic stirring in non-rotating substrates at room temperature. In some cases, during growth it has also been applied an external magnetic field of 100 Oe perpendicular to the sample plane. The growth time of NiFe was adjusted to reach the expected thicknesses by means of the Faraday's law:

$$C = \frac{nFd}{M_{atom}} St \quad (4)$$

where C is the electric charge measured in the cathode, n is the number of electrons involved in the reduction reaction, F is the Faraday's constant (96485,34C/mol), d is the density of the electrodeposited material, S is the area of the sample, t is the expected thickness, and M_{atom} is the molecular mass. In this work, thickness has ranged between 50 nm and 1.2 μ m for NiFe layers. For simplicity, we will denote as thick those samples with a thickness equal or larger than 800 nm, and thin those with a thickness below this value.

The electrolyte for $Ni_{90}Fe_{10}$ was water-based with a fixed pH of 2.2, and a composition of H_3BO_3 of 0.4 M, saccharine of 0.017 M, $NiSO_4$ of 0.7 M, and $FeSO_4$ 0.02 M, using a growth potential of -1.2 V in all cases.

We have used X-ray diffractometry (XRD) in the Bragg-Brentano configuration to study the structural properties. Measurements were performed in a D8 Brucker equipment using the Cu K_α wavelength (1.54056 Å). The composition of the layers has been obtained from energy dispersive X-ray spectroscopy (EDS) measurements performed in a JEOL JSM 6400 scanning electron microscope (SEM) working with an accelerator voltage of 20 kV. The experimental error for EDS measurements, ca. 1 at. %, has been inferred after averaging the composition measured in different regions of the samples. In-plane (IP) and OOP hysteresis loops were performed in a vibrating sample magnetometer (VSM) at room temperature. Magnetic Force Microscopy (MFM) measurements [21–22] were performed at ambient conditions using a custom modified system from Nanotec Electrónica S.L. The software WSxM [23] was used for data acquisition. This technique relies on the detection of the long-range magnetostatic force between the sample and a magnetic probe [24]. To detect the magnetic signal, it is necessary to perform two scans, one close to the surface to measure the topography and another one at typically 20–50 nm away from the surface to

minimize van der Waals interactions to detect only long-range magnetic interaction. Amplitude modulation (AM) method was carried out enabling the phase-locked loop (PLL) to track the resonance frequency of the oscillating cantilever and the magnetic signal was therefore recorded in the frequency shift channel, in Hz. Assuming that the tip-sample influence is negligible, the positive MFM contrast corresponds to a repulsive interaction, while the negative signal is due to an attractive interaction. In our experiments, the tip oscillates ~ 20 nm and the second scan was performed at a typical distance of 40 nm. Commercial probes from Budget Sensors MagneticMulti75-G, with CoCr coating were used.

3. Results and discussion

First of all, we have characterized the samples deposited on rigid substrates. The composition of the samples was measured by means of EDS being obtained $Ni_{90}Fe_{10}$ in all cases. For the identification of the XRD diffraction peaks we have used the cards 04-024-7186 ($Ni_{85}Fe_{15}$) and 00-004-0784 (Au). Apart from the reflections related to the Au buffer layer, the XRD patterns show the (111) and (200) diffraction peaks of NiFe (Fig. 1). The experimental position of the NiFe diffraction peaks is not affected either by magnetic stirring or when a magnetic field perpendicular to the sample plane is applied during growth.

To determine the lattice parameter (a) we have used the Bragg's law:

$$n\lambda_{rad} = 2d_{hkl}\sin\theta \quad (5)$$

where d_{hkl} is the distance between the family of planes with h , k , and l Miller indexes, θ the diffraction angle, and λ_{rad} the radiation wavelength (Cu K_α in this case). In the NiFe cubic system, we can obtain a from d_{hkl} since:

$$a = d_{hkl}\sqrt{(h^2 + k^2 + l^2)} \quad (6)$$

In all cases it is obtained a lattice parameter of 3.5 Å pretty close to the expected value extracted from the used XRD file 04-024-7186. Therefore, all the samples exhibit a similar strain state and effects related to an hypothetical magnetoelastic magnetic anisotropy is expected to be the same in all of them.

We have measured IP hysteresis loops to check the possibility of stripe domains in thick $Ni_{90}Fe_{10}$ layers grown in different conditions (Fig. 2a). Clearly, we can observe the fingerprint of this type of domains, the characteristic shape denoted as 'transcritical' [15,25], when layers are deposited without magnetic stirring. For thick films a perpendicular

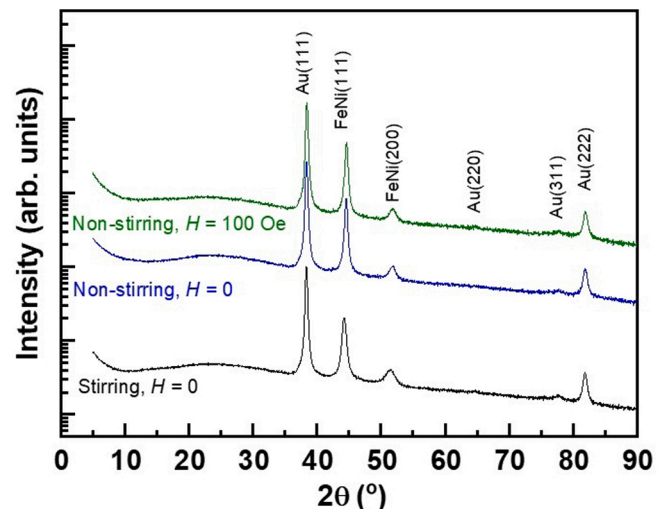


Fig. 1. XRD diffraction patterns of 1.2 μ m thick- $Ni_{90}Fe_{10}$ layers deposited under different growth conditions: stirring and $H = 0$, non-stirring and $H = 0$, non-stirring and $H = 100$ Oe. Curves have been shifted for clarity.

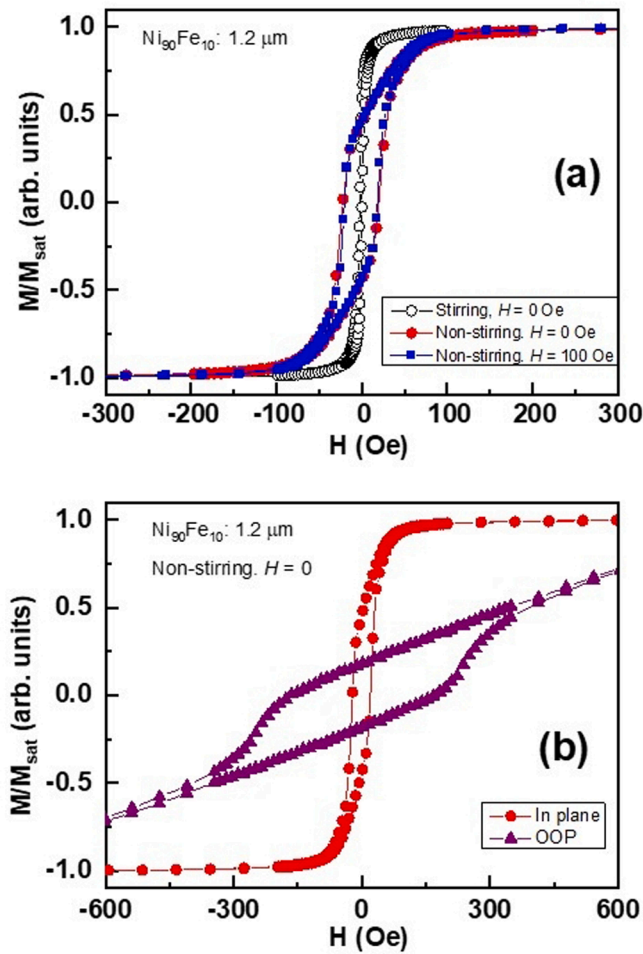


Fig. 2. (a) IP hysteresis loops for $1.2 \mu\text{m}$ thick- $\text{Ni}_{90}\text{Fe}_{10}$ layers deposited in different conditions: (○) stirring and $H = 0$, (●) non-stirring and $H = 0$ Oe, (■) non-stirring and $H = 100$ Oe. (b) IP (●) and OOP (▲) hysteresis loops for $1.2 \mu\text{m}$ thick- $\text{Ni}_{90}\text{Fe}_{10}$ layer deposited without an applied magnetic field and non-stirring conditions.

magnetic field of 100 Oe applied during growth does not have any significant effect on the transcritical shape of the IP hysteresis loop. On the contrary, a layer with the same thickness and composition but deposited in a magnetically stirred electrolyte, shows an IP hysteresis loop characteristic of a soft magnetic alloy without stripe domains. The existence of stripe domains in thick NiFe samples deposited without magnetic stirring have been confirmed by means of MFM (Fig. 3a). When the transcritical shape is present in the IP loops the remanence in the OOP loop is almost zero due to the presence of stripe domains [15]. In the studied samples (Fig. 2b), remanence is low although not completely null. The existence of some remanence in the OOP loops might be understood considering that the studied samples do not completely fulfill the requirement of the Murayama's model [26], that it is generally used to understand the formation of stripe domains. In that model, it is needed that the magnetization is aligned in the direction parallel to the stripes [26–27]. In the studied samples, some magnetization component misaligned with respect to the stripes direction can promote the observed remanence.

Considering our results and literature previously published in electrodeposited and sputtered Ni-Fe alloys [17,27–29], we can correlate the existence of stripe domains to the columnar growth. Moreover, our results indicate that in the considered as ‘thick’ thickness regime, equal or above 800 nm, stripe domains are not affected by a perpendicular magnetic field applied during growth. Therefore, the formation of stripe domains in thick $\text{Ni}_{90}\text{Fe}_{10}$ layers seems to be related to morphological

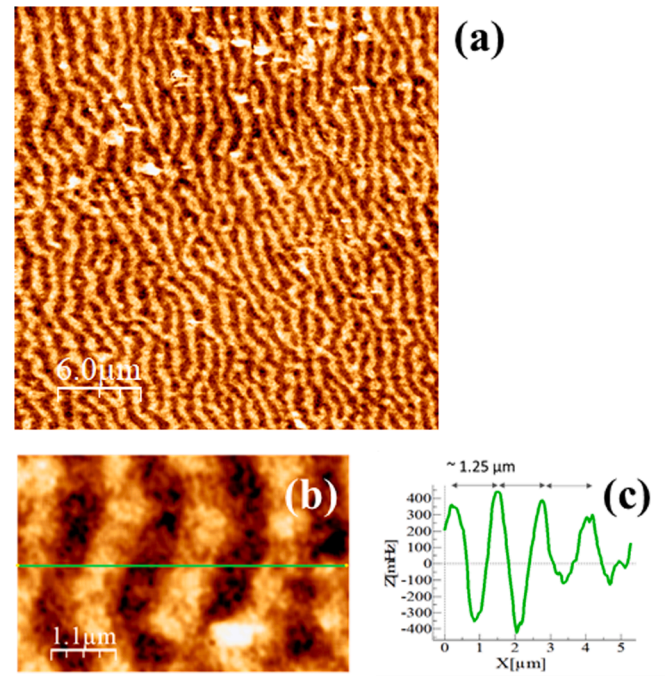


Fig. 3. (a) MFM image taken at remanence for $\text{Ni}_{90}\text{Fe}_{10}$ layers deposited in non-stirring and $H = 0$ conditions with a thickness of $1.2 \mu\text{m}$. Image size: $30 \mu\text{m} \times 30 \mu\text{m}$. (b) MFM image of a smaller area and its corresponding profile (c) where the stripe domain periodicity can be obtained.

effects promoted when the electrolyte is not stirred. Then, magnetic stirring is a fundamental growth parameter to tune stripe domains in this magnetic alloy as their formation is avoided upon its use. It has not been possible to check whether a perpendicular magnetic field can promote stripe domains formation in stirring conditions because this field affects magnetic stirring in our experimental set-up.

From the IP and OOP hysteresis loops of thick $\text{Ni}_{90}\text{Fe}_{10}$ layers it can be inferred the value of the perpendicular magnetic anisotropy and calculate both, the theoretical critical thickness and the quality factor. To obtain K_U we have followed the work of L. C. Garnier and coworkers [15]. First, we have quantitatively calculated K_U by measuring the area between the magnetization curves measured with the field in the IP and OOP directions. For thick layers deposited in non-stirring conditions either with and without a perpendicular applied magnetic field a K_U of around $500 \cdot 10^3 \text{ erg} \cdot \text{cm}^{-3}$ has been obtained. Considering the theoretical value for the saturation magnetization $M_{\text{sat}} = 590 \text{ emu} \cdot \text{cm}^{-3}$ [30], it is calculated a $Q = 0.023$ which means the layers have a moderate PMA. This is in agreement with the fact that periodicity of the stripe domains observed by MFM in these thick layers is similar to their thickness (Fig. 3b).

Introducing the experimental value for K_U in equation (3), and taking into account the reported value for $\text{Ni}_{90}\text{Fe}_{10}$, $A_{\text{ex}} = 1.4 \cdot 10^{-6} \text{ erg} \cdot \text{cm}^{-1}$ [30], it is calculated a $t_{\text{cr}} = 105 \text{ nm}$. This is an upper limit for t_{cr} considering the method used to calculate K_U . To check this value, we have deposited $\text{Ni}_{90}\text{Fe}_{10}$ layers with a thickness ranging from 50 nm to 600 nm, i.e. thin layers, in non-stirring conditions and without an external magnetic field. In these denoted as thin films, we have not found evidence of the transcritical shape in the IP hysteresis loops up to a thickness of at least 500 nm (Fig. 4). The inspection of the MFM images (Fig. 5) for these thin $\text{Ni}_{90}\text{Fe}_{10}$ samples reveals that even for a thickness of 600 nm, well above the theoretical critical thickness, it is obtained a contrast known as magnetic ripple [31–32] due to competing irregular magnetic anisotropies that promote an inhomogeneous magnetization. In fact, this magnetic ripple is also evident for a thickness of 600 nm (Fig. 5c) although this sample exhibits a clear transcritical shape in the IP hysteresis loops (Fig. 4b). Therefore, it seems that above the

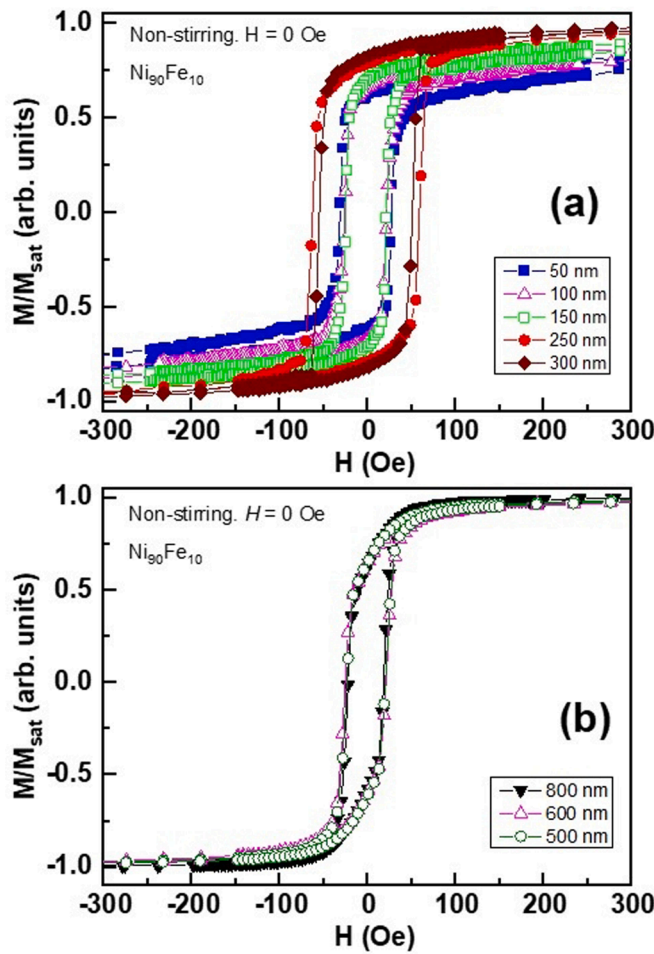


Fig. 4. IP hysteresis loops for $\text{Ni}_{90}\text{Fe}_{10}$ layers deposited in non-stirring and $H = 0$ conditions with thickness of (a) (■) 50 nm, (△) 100 nm, (□) 150 nm, (●) 250 nm, and (◆) 300 nm; (b) (○) 500 nm, (△) 600 nm, and (▼) 800 nm.

theoretical t_{cr} of 105 nm it is first developed a magnetic ripple because the PMA is not large enough to counterbalance other sources of magnetic anisotropy present in the layers. In fact, stripe domains start to be visible by MFM for a thickness of 800 nm that is pretty large in comparison to the theoretical t_{cr} (Fig. 5d). Therefore, it is needed a much higher thickness than the theoretical critical value to observe by MFM stripe domains. This difference between experimental results and the theoretical prediction can be understood considering that the expression of $t_{cr} = 2\pi\sqrt{A_{ex}/K_U}$ was obtained within the framework of Murayama's model considering that the local magnetization does not change its direction with respect to the direction parallel to the stripes [26–27]. The magnetic ripple observed by MFM reflects the presence of random sources of anisotropy that can misalign the magnetization being therefore the Murayama's model no longer valid.

Finally, to check the quality of the thick $\text{Ni}_{90}\text{Fe}_{10}$ layers from the magnetoelastic point of view, we have inferred the value of λ following a routine reported in previous works [33–35]. Since the samples studied in this work are polycrystalline, this method can provide an average value for λ . To do that, a 1.2 μm -thick $\text{Ni}_{90}\text{Fe}_{10}$ layer was grown in non-stirring conditions and without a perpendicular magnetic field on top of an outward bent 150 μm -thick kapton substrate with a radius curvature of $\rho = 3.42$ cm that promoted a compression state in the released layers as sketched in Fig. 6a. To check whether the use of flexible substrates affects the magnetic properties, we have deposited as a sample of reference a 1.2 μm -thick $\text{Ni}_{90}\text{Fe}_{10}$ layer on top of a non-bent kapton substrate. In comparison with thick layers deposited on rigid glass

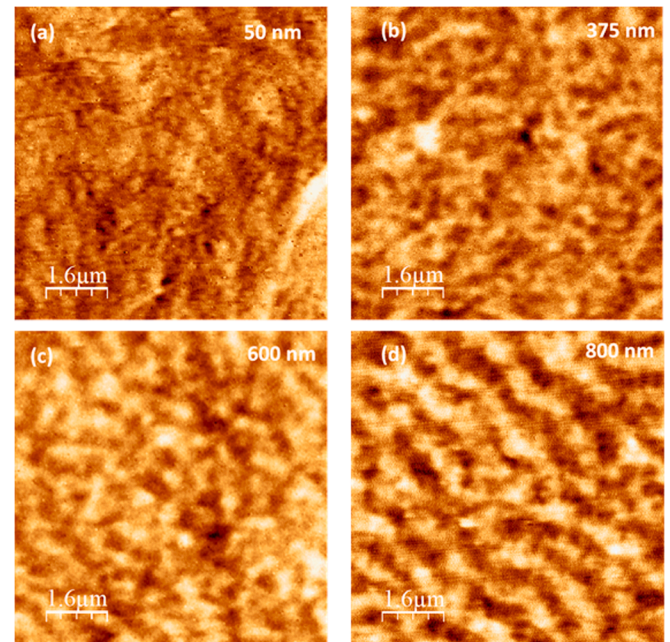


Fig. 5. MFM images taken at remanence for $\text{Ni}_{90}\text{Fe}_{10}$ layers deposited in non-stirring and $H = 0$ conditions with thickness of (a) 50 nm, (b) 375 nm, (c) 600 nm and (d) 800 nm. Images size: 8 $\mu\text{m} \times 8 \mu\text{m}$.

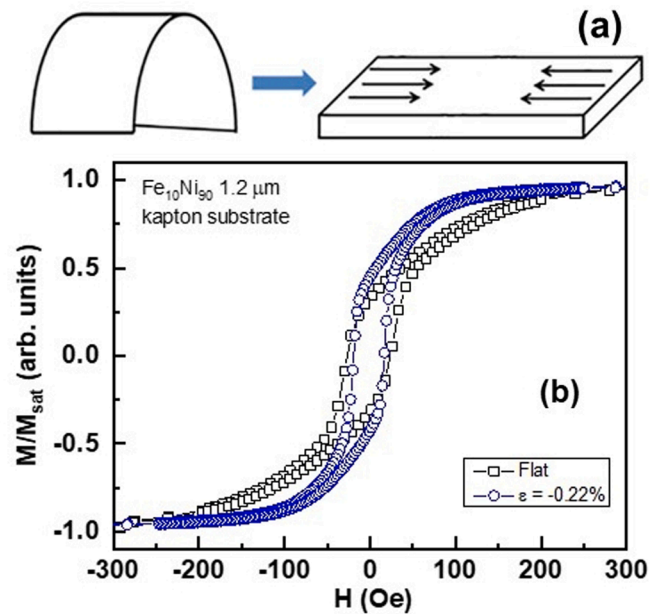


Fig. 6. (a) Scheme of the design use to electrodeposit on top of outward bent kapton/Au substrates that promote an in-plane compressive stress when the layers are released after growth. (b) IP hysteresis loops of $\text{Ni}_{90}\text{Fe}_{10}$ layers deposited on flexible kapton/Au (□) flat and (○) outward bent substrates.

substrates, this sample exhibits a small decrease of K_{OOP} from $500 \cdot 10^3$ erg/cm^3 to $455 \cdot 10^3$ erg/cm^3 but with a transcritical shape still visible in the IP hysteresis loop (Fig. 6b).

The induced mechanical deformation (ε) after the release of the sample deposited in the outward bent substrate is:

$$\varepsilon = \frac{h}{2\rho} \quad (7)$$

Then, in our particular geometry (Fig. 6a) and for a h that considers

the thickness of both substrate (150 μm) and NiFe layer (1.2 μm) it is promoted a compression deformation of $\varepsilon = -0.002$ with a compressive stress (σ):

$$\sigma = \frac{\varepsilon E_f}{1 - \nu^2} \quad (8)$$

where E_f and ν are the Young's modulus and Poisson ratio of the NiFe layer, respectively. In this case, the values are $E_f = 180$ GPa and $\nu = 0.3$ [36]. Due to this IP compressive stress, it is induced an IP magnetoelastic anisotropy, that decreases the perpendicular anisotropy to $263 \cdot 10^3$ erg/cm³. From a linear fit to the expression [1–2]:

$$K = \frac{3}{2} \lambda \sigma \quad (9)$$

in which K is the magnetic anisotropy of compressed and non-compressed layers grown on flexible substrates, it is inferred a λ of -22 ppm, pretty close to the reported value in the bulk alloy.

Therefore, this investigation demonstrates the possibility of using the electrodeposition technique to fabricate magnetoelastic Ni₉₀Fe₁₀ films in which the PMA can be tuned thanks to the mechanical deformation.

4. Conclusions

In summary, we have successfully demonstrated the capability of using the electrodeposition technique to grow high-quality magnetoelastic Ni₉₀Fe₁₀ films. Magnetic stirring appears as a fundamental growth parameter since it avoids the formation of stripe domains. In NiFe samples that exhibit stripes, we have obtained an experimental value of K_U of around $500 \cdot 10^3$ erg/cm³ which promotes a moderate PMA with a $Q = 0.023$ and a critical thickness of 105 nm. However, above this theoretical critical thickness it is first obtained a magnetic ripple that evolves to stripe domains when the thickness is at least 800 nm in order that the PMA can counterbalance other sources of random magnetic anisotropy. Finally, layers with stripe domains also present a high quality from the magnetoelastic point of view as reflected by the λ of around -22 ppm that has been measured in the studied samples.

Declaration of Competing Interest

The authors declare that they have no known competing financial interests or personal relationships that could have appeared to influence the work reported in this paper.

Data availability

Data will be made available on request.

Acknowledgements

This work has been financially supported through the projects RTI2018-097895-B-C43 (FEDER) of the Spanish Ministry of Science, Innovation, and Universities, PID2021-122980OB-C51, PID2021-122980OA-C53 (FEDER) of the Spanish Ministry of Science and Innovation and SI1/PJ1/2019-00055 of the Regional Government of Madrid and within the framework of the agreement with the Autonomous University of Madrid: *Excelencia para el Profesorado Universitario*. Financial support from the Plan Propio of Universidad Castilla-La Mancha (FEDER, EU) for the “Grupo de Materiales Magnéticos (GMM)” is also acknowledged.

The data that support the findings of this study are available from the corresponding author upon reasonable request.

References

- [1] S. Chikazumi, Physics of ferromagnetism, Oxford University Press, 1997.
- [2] E. du Trémolet de Lacheisserie, Magnetism, EDP Sciences, 2000.

- [3] D. Petti, S. Tacchi, E. Albisetti, Review on magnonics with engineered spin textures, J. Phys. D: Appl. Phys. 55 (2022), 293003.
- [4] B. Casals, N. Statuto, M. Foerster, A. Hernández-Mínguez, R. Cicheler, P. Manshausen, A. Mandziak, L. Aballe, J.M. Hernández, F. Maciá, Generation and imaging of magnetoacoustic waves over millimeter distances, Phys. Rev. Lett. 124 (2020), 137202.
- [5] M. Foerster, F. Maciá, N. Statuto, S. Finizio, A. Hernández-Mínguez, S. Lendínez, P. V. Santos, J. Fontcuberta, J.M. Hernández, M. Kläui, L. Aballe, Direct imaging of delayed magneto-dynamic modes induced by surface acoustic waves, Nature Comm. 8 (2017) 407.
- [6] A. Hernandez-Minguez, F. Macia, J.M. Hernandez, J. Herfort, P.V. Santos, Large non-reciprocal propagation of surface acoustic waves in epitaxial ferromagnetic/semiconductor hybrid structure, Phys. Rev. Appl. 13 (2020), 044018.
- [7] H. Qin, R.B. Holländer, L. Flajsman, S. van Dijken, Low-loss nanoscopic spin-wave guiding in continuous yttrium iron garnet films, Nano Letter. 22 (2022) 5294–5300.
- [8] P. Gruszecki, K.Y. Guslienko, I.L. Lyubchanskii, M. Krawczyk, Inelastic spin-wave beam scattering by edge-localized spin waves in ferromagnetic thin film, Phys. Rev. Appl. 17 (2022), 044038.
- [9] F. Zhuo, H. Li, Z. Cheng, A. Manchon, Magnonic metamaterials for spin-wave control with inhomogeneous Dzyaloshinskii-Moriya interactions, Nanomaterials 12 (2022) 1159.
- [10] T. Böttcher, M. Ruhwedel, K.O. Levchenko, Q. Wang, H.L. Chumak, M.A. Popov, I. V. Zavislyak, C. Dubs, O. Surzhenko, B. Hillebrands, A.V. Chumak, P. Pirro, Fast long-wavelength exchange spin waves in partially compensated Ga:YIG, Appl. Phys. Lett. 120 (2022), 102401.
- [11] C. Liu, S. Wu, J. Zhang, J. Chen, J. Ding, J. Ma, Y. Zhang, Y. Sun, S. Tu, H. Wang, P. Liu, C. Li, Y. Jiang, P. Gao, D. Yu, J. Xiao, R. Duine, M. Wu, C.-W. Nan, J. Zhang, H. Yu, Current-controlled propagation of spin waves in antiparallel, coupled domains, Nature Nanotech. 14 (2019) 691.
- [12] J. Ben Youssef, N. Vukadinovic, D. Billet, M. Labrune, Thickness-dependent magnetic excitations in Permalloy films with nonuniform magnetization, Phys. Rev. B 69 (2004), 174402.
- [13] M. Liu, S. Du, F. Wang, R. Adam, Q. Li, X. Ma, X. Guo, X. Chen, J. Yu, Y. Song, J. Xu, S. Li, D. Cao, Influence of surface pinning in the domain on the magnetization dynamics in permalloy striped domain films, J. Alloys Compd. 869 (2021), 159327.
- [14] M. Liu, Q. Li, C. Song, H. Feng, Y. Song, L. Zhong, L. Pan, C. Zhao, Q. Li, J. Xu, S. Li, J. Wang, Q. Liu, D. Cao, Microwave excitations and hysteretic magnetization dynamics of stripe domain films, J. Magn. Magn. Mater. 547 (2022), 168939.
- [15] L.-C. Garnier, M. Marangolo, M. Eddrief, D. Bisero, S. Fin, F. Casoli, M.G. Pini, A. Rettori, S. Tacchi, Stripe domains reorientation in ferromagnetic films with perpendicular magnetic anisotropy, J. Phys.: Matter 3 (2020), 024001.
- [16] A. Hubert, R. Schäfer, Magnetic domains: the analysis of magnetic microstructures, Springer Science & Business Media, 2008.
- [17] M. Romero, R. Ranchal, D. Ciudad, M. Maicas, C. Aroca, Magnetic properties of sputtered permalloy/molybdenum multilayers, J. Appl. Phys. 110 (2011), 083910.
- [18] D. Markó, F. Valdés-Bango, C. Quirós, A. Hierro-Rodríguez, M. Vélez, J.I. Martín, J. M. Alameddine, D.S. Schmool, L.M. Álvarez-Prado, Tunable ferromagnetic resonance in coupled trilayers with crossed in-plane and perpendicular magnetic anisotropies, Appl. Phys. Lett. 115 (2019), 082401.
- [19] M. Ciriá, K. Ha, D. Bono, R.C. O'Handley, Magnetoelastic coupling in epitaxial Cu/Ni₉₀Fe₁₀/Cu/Si(001) thin films, J. Appl. Phys. 91 (2002) 8150–8152.
- [20] M. Ciriá, R.C. O'Handley, Surface- and strain-induced anisotropy in epitaxial Cu/Ni₉₀Fe₁₀/Cu/Si(001) films, J. Magn. Magn. Mater. 240 (2002) 464–466.
- [21] Y. Martin, H.K. Wickramasinghe, Magnetic imaging by “force microscopy” with 1000 Å resolution, Appl. Phys. Lett. 50 (1987) 1455–1457.
- [22] J.J. Sáenz, N. García, P. Grütter, E. Meyer, H. Heinzelmann, R. Wiesendanger, L. Rosenthaler, H.R. Hidber, H.-J. Güntherodt, Observation of magnetic forces by the atomic force microscope, J. Appl. Phys. 62 (1987) 4293–4295.
- [23] I. Horcas, R. Fernández, J.M. Gómez-Rodríguez, J. Colchero, J. Gómez-Herrero, A. M. Baró, WSXM: A software for scanning probe microscopy and a tool for nanotechnology, Rev. Sci. Instrum. 78 (2007), 013705.
- [24] O. Kazakova, R. Puttock, C. Barton, H. Corte-León, M. Jaafar, V. Neu, A. Asenjo, Frontiers of magnetic force microscopy, J. Appl. Physics 125 (2019), 060901.
- [25] N. Saito, H. Fujiwara, Y. Sugita, A new type of magnetic domain structure in negative magnetostriction Ni-Fe films, J. Phys. Soc. Jpn. 19 (1964) 1116–1125.
- [26] Y. Murayama, Micromagnetics on stripe domain films. I. Critical cases, J. Phys. Soc. Japan 21 (1966) 2253–2266.
- [27] A.V. Svalov, A.N. Gorkovenko, A. Larrañaga, M.N. Volochaev, G.V. Kuryandinskaya, Structural and magnetic properties of FeNi films and FeNi-based trilayers with out-of-plane magnetization component, Sensors 22 (2022) 8357.
- [28] D. Cao, Z. Wang, E. Feng, J. Wei, J. Wang, Q. Liu, Magnetic properties and microstructure investigation of electrodeposited FeNi/TTO films with different thickness, J. Alloys Compd. 581 (2013) 66–70.
- [29] Q. Li, Y. Song, F. Wang, M. Liu, X. Ma, X. Guo, X. Chen, J. Yu, S. Du, H. Li, J. Xu, S. Li, D. Cao, Perpendicular magnetization anisotropy induced dynamical coherence reduction in stripe domain film, J. Phys.: Cond. Matter 34 (2022), 155802.
- [30] E. V. Kudyukov, A. S. Bolyachkin, K. G. Balymov, V. O. Vas'kovskiy, Micromagnetic modeling of tensor magnetoresistance effect in films with unidirectional anisotropy, AIP Conference Proceedings 1886 (2017) 020014.
- [31] P. Bartolomé, M. Maicas, R. Ranchal, Out of plane component of the magnetization of sputtered Fe₇₂Ga₂₈ layers, J. Magn. Magn. Mater. 514 (2020), 167183.
- [32] A. Begué, M.G. Proietti, J.I. Arnaudas, M. Ciriá, Magnetic ripple domain structure in FeGa/MgO thin films, J. Magn. Magn. Mater. 498 (2020), 166135.

- [33] I. Hontecillas, I. Figueruelo, S. Abad, R. Ranchal, Tuning the magnetic anisotropy of Ga-rich FeGa thin films deposited on rigid substrates, *J. Magn. Magn. Mater.* 494 (2020), 165771.
- [34] G. Dai, Q. Zhan, H. Yang, Y. Liu, X. Zhang, Z. Zuo, B. Chen, R.-W. Li, Controllable strain-induced uniaxial anisotropy of $\text{Fe}_{81}\text{Ga}_{19}$ films deposited on flexible bowed substrates, *J. Appl. Phys.* 114 (2013), 173913.
- [35] Y. Yu, Q. Zhan, J. Wei, J. Wang, G. Dai, Z. Zuo, X. Zhang, Y. Liu, H. Yang, Y. Zhang, S. Xie, B. Wang, R.-W. Li, Static and high frequency magnetic properties of FeGa thin films deposited on convex flexible substrates, *Appl. Phys. Lett.* 106 (2015), 162405.
- [36] H. Ren, E. Gerhard, Design and fabrication of a current-pulse-excited bistable magnetic microactuator, *Sens. Actuator A Phys.* 58 (1997) 259–264.